

ASSESSING THE ABILITY OF ROOF-MOUNTED PHOTOVOLTAIC ARRAYS AND A BUFFERING BATTERY TO SUPPORT URBAN ELECTRIC VEHICLE CHARGING

N J Kelly¹, J Allison², G Flett¹, J W Hand¹

¹ Energy Systems Research Unit, University of Strathclyde, Glasgow, Scotland

²Arbnco Ltd, Inovo Building, George St, Glasgow, Scotland

Abstract

This paper reports on an analysis of a proposed EV charging hub at a city centre car park in Glasgow Scotland, equipped with a 200kWp roof-mounted photovoltaic (PV) array and buffering battery. Specifically, the ability of the PV plus battery to mitigate the impact of EV charging on energy networks and the environment was assessed. The car park performance was simulated over a calendar year using building simulation and supporting tools. The analysis featured a range of vehicles using the hub (10 - 500) and a range of supporting battery sizes (0-500kWh). The results indicated that supporting batteries of 10kWh or less, increased the utilisation of PV generated electricity and decreased the electrical energy exchanges with the grid. Larger batteries produced marginal gains in performance. With a load of less than 100 vehicles using the hub, peak power imports from the grid reduced with increasing battery size; battery size had a minimal effect above this load level. Peak exported power reduced with increasing battery size if more than 200 vehicles used the hub. Below this load level, the number of vehicles and battery size made a minimal difference. In operation, the PV and battery-supported-hub was carbon neutral or carbon positive when servicing up to 200 EVs.

Introduction

In common with most of the rest of the developed world, the UK aims to be carbon neutral by 2050 (UK Government, 2019) and a central plank of its decarbonisation strategy is the decarbonisation of transport, with petrol and diesel vehicles scheduled to be phased out by 2035 (DFT, 2018). The primary means to achieve this is through the decarbonisation of grid electricity, coupled with a rapid uptake of electric vehicles (EVs) or vehicles fuelled by hydrogen from electrolysis. Of the two, electric vehicles are currently far closer to mass market adoption (Kulagin & Grushevenko, 2020), though this situation may change in the longer term. This paper looks at the issues surrounding a growth in publicly charged EVs in urban areas in the short-to-medium term. Specifically, the energy and environmental performance of an EV charging hub supported by a rooftop PV array and buffering battery was analysed. This system is being developed in Glasgow, Scotland, as part of the EU-funded RUGGEDISED project (<http://www.ruggedised.eu/>). The charging hub is one of

a range of low carbon, “smart” solutions that are being demonstrated in several European cities. The hub is located at a car park close to Glasgow city centre. The building has 1170 parking spaces located over 9 floors. The PV rooftop array, already designed for installation, has a notional peak power output of 200kWp and comprises 625 PV panels, with a total surface area of 1250m². The panels are tilted at 20° to the horizontal (GCC, 2018).



Figure 1: Duke St car park (Image: Google street view).

Mitigating the impacts caused by the growth of EVs is of interest to policy makers and utilities, as increasing charging demand (along with the electrification of heat and increased use of cooling in a warming climate) poses a significant challenge for urban energy networks, with the risk that increasing demand for electricity could outstrip the development of the infrastructure required to support it. This could lead to the need for extensive investment and upgrading of power networks to combat potential supply problems (Earl & Fell, 2019). There is also the risk of increased greenhouse gas emissions, as rapid growth in the use of electrical energy could result in growing use of backup fossil fuel generation (Bahamonde-Birke, 2020). The use of photovoltaics to support daytime charging of electric vehicles (EV) is of interest as there is, in theory, a strong temporal match between the timing of the demand and the availability of the zero-carbon solar electricity.

There have been some previous studies investigating aspects of the energy, environmental and economic performance of PV supported EV charging (e.g. Bhatti et al, 2016). In an early US study, Birnie (2009) undertook some high-level modelling, indicating that for commuters in the north-eastern USA, the energy produced by 15m²

of PV could entirely offset the energy required for commutes of 15-30 km in PHEV vehicles. Mouli *et al.* (2016) analysed the performance of a small PV system (10kWp) supporting the charging of up to 3 vehicles in the Netherlands. The EV charge taken was assumed to be a fixed 10kWh, though various charging profiles are analysed; the use of even a small 10 kWh battery was seen to significantly reduce energy drawn from the grid. Several studies have assessed the ability of intelligently controlled charging to further mitigate grid impacts. For example, Tupule *et al.* (2013) analysed a 100kW PV array supporting up to 50 electric vehicles in different US cities along with the use of smart charging control. They demonstrated a significant reduction in CO₂ emissions; the use of a buffering battery was not considered. Chaudhari *et al.* (2018), utilized a linear programming approach in a least cost optimization of an EV charging hub in Singapore featuring photovoltaics (PV) and battery storage. The authors concluded that the use of PV plus storage could reduce the average and peak power demand from EV charging.

This research takes a slightly different approach to these latter papers and does *not* look at demand side restrictions on charging through active charge control or the potential for vehicle-to-grid operation. Instead, a local supply-side solution is assessed. Specifically, ability of PV with local battery storage to mitigate the effects of unconstrained charging is examined for different supporting battery sizes and populations of vehicles. The rationale behind this approach was that 1) at least in the short-term, intelligent control of vehicle charging will lag the deployment of charging infrastructure and so the work here represents the analysis of a likely-near-term scenario; 2) local, supply-side approaches to controlling EV charging impacts on the grid such as PV with batteries could be seen to be preferable to demand-side, time-based charge control for time-constrained users of public charge points; 3) most of the papers reviewed analysed fixed vehicle numbers and battery sizes; and 4) constraining stochastic demand for power through control (intelligent-or-otherwise) can lead to unintended demand peaks, worsening rather than exacerbating the impact on the grid (e.g. Callaway, 2009).

AIM

This paper assesses the contribution that building-mounted photovoltaics with battery storage could make to mitigate the impact of increased public, urban EV charging on electricity networks and the wider environment. The impact of local renewable electricity production on the energy exchanged with the electrical network, peak electrical power flows and emissions is analysed for a variety of operating conditions.

Contribution

A new empirically derived statistical model for the prediction of public EV charging demand is presented. A wide-ranging sensitivity analysis is undertaken to quantify the impact that PV plus different supporting battery sizes could have in mitigating the detrimental effects that EV charging on the local electricity network.

The carbon emissions associated with the different cases modelled are also analysed using time-varying grid carbon intensity figures.

METHOD

A multi-tool modelling approach was adopted.

- 1) The open source ESP-r building simulation tool (ESRU, 2020) was used to calculate the time-varying output of a 200kWp roof-mounted PV array at the Duke Street car park; the output was a PV power supply profile.
- 2) A probabilistic EV charging model for public hubs, developed specifically for the work reported here, was used to calculate the electrical demand associated with a fleet of electric vehicles using the hub during the day. The output of the model was a set of time-series power demand profiles for different numbers of EVs.
- 3) A custom load-flow model of the charging hub was created that included battery storage and that featured ability to apply a supportive battery operating strategy. The tools above were used to quantify the interactions between the grid, battery storage, PV generation and EV charging hub.

Car Park Model

The ESP-r model features a detailed representation of the car park and PV array (Figure 2). ESP-r includes integrated thermal and electrical algorithms for simulating the performance of building-integrated PV (Kelly, 1998). These make use of the tool's intrinsic thermal and solar processing capabilities to calculate the electrical power output.

The PV array is represented explicitly as a set of building surfaces. When the model is simulated using real climate data (temperature, solar radiation, wind speed and direction) as a boundary condition over a user defined period, the time-varying PV array temperature can be computed. This is based on a surface energy balance using the computed transient energy exchanges: the surface conduction, convective and infrared heat transfers, incident direct, diffuse and ground reflected solar radiation.

The corresponding electrical algorithm (based on Equation 1) solves the output voltage and current of a single PV cell as a function of the computed total surface-incident solar radiation intensity $\dot{Q}_{i,SOL}$ (which includes the effects of shading), and the array surface temperature T_i . The results are then extrapolated to determine the operating state of the panel and hence the whole array, assuming all the panels are of the same type and at the same orientation and tilt.

$$P_i = \left[V_i I_G \left(1 - \exp\left(\frac{eV_i}{\lambda k T_i}\right) \right) - V_{MP} I_L \right] n m q \quad (1)$$

The power output of the PV array is passed back to the surface thermal energy balance resulting in the PV surface temperature being suppressed when the PV is producing power (as happens in reality). The input data for the PV model is shown in Table 1.

ESP-r and its PV model has been extensively validated, as summarized by Strachan *et al.* (2008).



Figure 2: rendered model of the ESP-r Duke St Car Park model with roof-mounted PV arrays.

Table 1: characteristics of the PV panels used in the analysis [19].

Open circuit voltage (V_{OC})	42.2 V
Short circuit current. (I_{SC})	7.15 A
Voltage at maximum power point (V_{MP})	34.3 V
Current at maximum power point (I_{MP})	6.72 A
Reference insolation (\dot{Q}_{ref})	1000 W/m ²
Reference temperature (T_{ref})	298 K
Number series connected cells in a branch (n)	72
Number parallel connected branches (m)	1
Number of panels (q)	625
Temperature sensitivity of I_G (β)	1.072

An example of calculated PV power output over a simulated year is as shown in Figure 3.

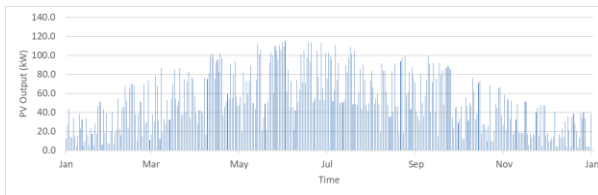


Figure 3: simulated car park half-hourly PV output.

It is worth noting that although the array mounted on the car park roof has a notional output of 200kW_p, the simulated peak power produced was significantly less than this at around 115 kW. The main reasons for this are that 1) the incident solar radiation on the PV is always less than that used by manufacturers in tests to determine the notional power output; 2) during these tests the panel temperature is held to 25°C, however the operating temperature of insolate panels is typically higher than this, reducing operating efficiency and further reducing power output; 3) the model also includes converter inefficiencies (~10%). This reduction in real-life performance compared to

manufacturers' tests has been noted elsewhere (Clarke et al, 1996).

EV Charging Model

For a user-defined population of vehicles, the model calculates the total charging demand at half hour time intervals for a population of vehicles. It was calibrated using a Transport Scotland dataset (Transport Scotland, 2018) containing information on all public EV charge point use in Scotland between 2015 and 2018. The dataset included the identity of the vehicle charging, the charger id and geographical location, the charger type and capacity, the charging date, the connection and disconnection times, the charge taken and the charge cost. For a user defined period, and for each vehicle, the calibrated calculated:

- whether the vehicle would charge on a particular day;
- time at which the vehicle would charge;
- whether there was a compatible charge point available at the specified charge time;
- and the charge taken (kWh) during a charging event (which dictated the duration of the charge, along with the charger power).

To determine whether a vehicle would charge on a specific day, the dataset was analysed to determine a charging behaviour for each vehicle at the beginning of the simulation process. This behaviour indicated how often (on average) a vehicle would charge per week. For each vehicle using the hub, a random value (r_w) between 1-100 was generated and compared to the cumulative probability, p_w , (shown in Figure 4); this then determined the vehicle's average number of charge events per week and consequently the daily probability (p_d) of a charge event occurring.

For example, if a vehicle was determined to charge on average twice per week, then the daily probability of charging was 28.6%. Once set, the charging behaviour and daily charging probability for each individual vehicle remained the same over the simulated period.

To test if a vehicle charged on a specific day, a further random value (r_d) was generated and compared to the daily charging probability, then if $r_d \leq p_d$ the vehicle would charge on that day.

To identify the time at which a vehicle charged, the Transport Scotland dataset was used to generate two further curves describing the cumulative probability of a charge event starting on a day that an EV charges for weekdays and weekends, respectively. The data showed that charging behaviour was markedly different for each. The curves are shown in Figure 5.

To determine when a charge event started, a random test value (r_s) 1-100 was generated and compared to the appropriate cumulative probability value p_s at 30-minute time intervals throughout the day. When $p_{s,t} < r_t \leq p_{s,t+30}$ the charging was deemed to start in that time interval.

When a vehicle charged, the amount of charge taken was determined using a similar approach taken to determining the charge start time and used another correlation derived

from the Transport Scotland dataset (*ibid*) and shown in Figure 6.

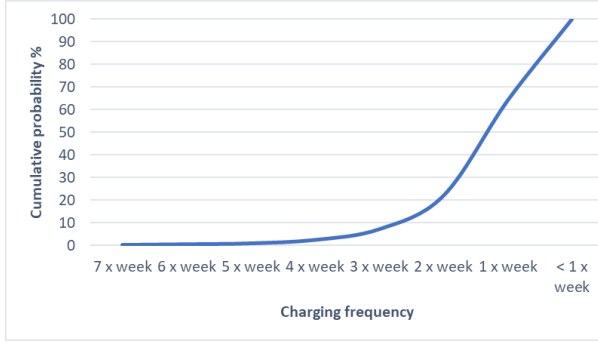


Figure 4: cumulative probability (expressed as a %) of vehicle charge events per week.

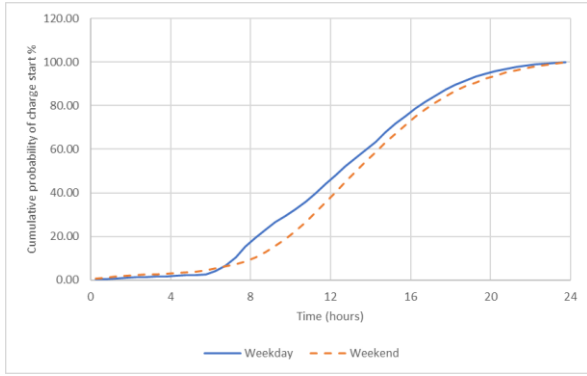


Figure 5: cumulative probability of charge starting.

The time taken to charge was then the charge taken divided by the power of the charger to which the vehicle is connected.

Charging Hub Electrical Model

To assess the interaction between the PV, battery, charging load and the network, an electrical network model was developed; this treated the car park as a single bus-bar system, with the PV, EV demand and a battery all connected via converters to a common AC busbar, which also included a (bi-directional) connection to the local LV grid.

The instantaneous EV demand and PV generation were obtained from the profiles illustrated in Figure 7 and Figure 3, respectively. The battery power flows were also bi-directional in that it could either charge from, or discharge to the busbar. The battery can reconcile short term-temporal mismatches between the availability of PV-generated electricity and vehicle charging.

An example of a demand profile generated by the tool is shown in Figure 7.

The basic equation for the determining power exchanged between the different elements the PV-EV system were as follows.

$$P_{LV} = P_{EV} - P_{PV} \pm P_B \quad (2)$$

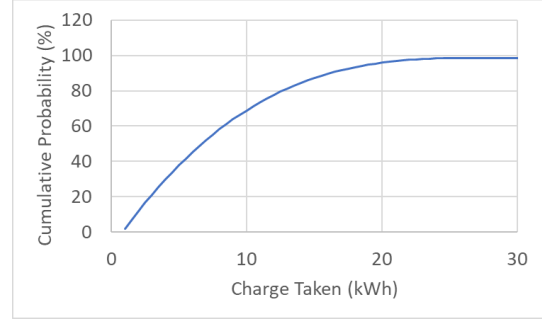


Figure 6: cumulative probability of energy taken during a charge.

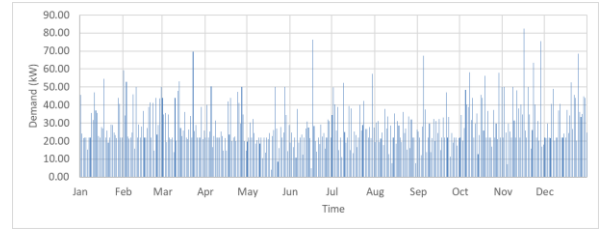


Figure 7: example of demand profile for a fleet of 50 electric vehicles serviced by the hub.

The model tracked the battery state of charge using the following equations.

$$C_B(t + \Delta t) = (1 - \epsilon)C_B(t) \pm P_B \quad (3)$$

$$SOC_B = \frac{C_B(t + \Delta t)}{C_{B MAX}} \quad (4)$$

The battery power flow, P_B , was determined by the battery operating strategy. If there was available energy from the PV, and the total vehicle charging demand, P_{EV} , was less than the PV generation, P_{PV} , then the battery charged. Where the PV output power exceeded the battery's maximum charging rate, then the surplus was spilled to the grid. If there was energy available from the PV, but this was less than the charging demand, then the battery discharged to help meet the demand, if there was sufficient charge in the battery. Only where the PV and battery were insufficient to meet the EV demand was power drawn from the grid.

$$P_B = \begin{cases} \eta_c \eta_x (P_{PV} - P_{EV}), & \text{if } SOC_B < 1 \wedge P_{PV} > P_{EV} \\ \frac{P_{PV} - P_{EV}}{\eta_D \eta_x}, & \text{if } SOC_B > SOC_{MIN} \wedge P_{PV} < P_{EV} \\ 0 & \text{otherwise} \end{cases} \quad (5)$$

SIMULATIONS

To quantify the energy and environmental performance of the car park charging hub, its operation was simulated over two calendar years. This involved generating a two-year time series profile of PV array output and two-year demand time series profile for different numbers of EVs. The first year of data was used for pre-simulation and only the second year's data was used in the analysis. This was done to ensure that the SOC of the battery at the beginning

of the simulated period was based on calculated values and not a guestimate, as (particularly for larger battery sizes) the starting SOC had an impact on the annual results.

Table 1: Battery parameters used with the model (GCC,2018).

battery capacity (C_{MAX})	0 – 500 kWh
minimum state of charge (SOC_{MIN})	0.2
charging efficiency (η_C)	0.960
discharge efficiency (η_D)	0.972
battery standing loss (ϵ)	6.25E-5 of $C_B(t)$ per time step
converter efficiency (η_X)	0.9

Table 2: charger “fleet” used with the model (GCC, *ibid*).

charger power (kW)	charge points (-)	number of chargers (-)
7 (AC)	1	4
22 (AC)	2	5
50 (DC)	1	5

To assess the impact that the numbers of EVs using the hub and the battery size had on performance, the following parameters were explored:

- the vehicles supported by the hub were varied between 0 and 500; the car park has around 1200 spaces. With an average occupancy of 82% (City Parking, 2015), 500 EVs represents approximately half of all vehicles using the car park; a scenario not likely to occur until the late 2030’s given current projections (Hirst, 2020).
- the battery size was varied between 0 and 500 kWh; the upper value is sufficient to store the maximum daily electrical output from the PV array.

In total, 80 operating cases were analysed; in all of these, it was assumed that there would be enough chargers to meet the needs of any vehicles using the hub; the validity of this assumption is discussed later. Further, as an objective was to assess peak power flows, no limits were set on the power that could be drawn from or exported to the network and the power that could be accepted by or discharged from the battery.

The metrics extracted from each simulation were as follows.

- The fraction of vehicle charging load that was supplied by the PV - the renewable utilization fraction (RUF); the higher value of RUF, the more local, zero-carbon electricity is being used to charge vehicles, rather than being drawn from the grid.
- The energy exchanges with the grid; this information was used to calculate the carbon emissions associated with the charging hub.
- The peak power imported or exported to the electricity network; the latter has an impact on the

viability of the EV charging hub scheme, as higher the peak power flows require a larger investment in infrastructure to support charging and may require that the surrounding network is reinforced.

- The state of charge (SOC) and power flows associated with the battery; this is useful in determining a best-fit battery size to support EV charging and understanding the characteristics of electrical power and energy exchanges with the network.

RESULTS AND DISCUSSION

The total annual energy from the PV array, after conversion was approximately 110 MWh. The total simulated demand for the different numbers of vehicles using the charging hub is as shown in Table 3.

Table 3: annual simulated electrical demand with different numbers of vehicles using the hub¹.

Vehicles	10	50	100	200	350	500
Demand (MWh)	4.8	36.8	62.6	115.4	195.0	272.9

The results indicate that the net public charging demand of a vehicle fleet of just under 200 EVs could be fully offset by the 200kWp PV array of the car park. Note however, that this does not include the energy demand associated with the home charging of these vehicles.

The Renewable Utilisation Fraction (RUF) was calculated as follows:

$$F = 1 - \frac{\text{Annual Imported Energy (kWh)}}{\text{Annual Energy Demand (kWh)}} \quad (6)$$

Figure 8 shows the renewable utilization fraction (RUF) for vehicle numbers between 10-500 and battery sizes between 0-500kWh.

As the size and capacity of the car park PV array was fixed, the renewable utilisation fraction dropped as the vehicle demand increased. For example, with a 100kWh battery, 100% RUF was achievable for a 10-vehicle load, but only around 40% was achievable with 500 vehicles.

The addition of a relatively small size of battery (less than 10 kWh), significantly improved the localized use of the PV generated power. For example, with 10EVs using the hub, the RUF was approximately 58% with no battery, rising to 100% with a 5kWh battery. Similarly, with 200 EVs using the hub the RUF increased from 43% with no battery to almost 63% with a 10 kWh supporting battery.

Adding additional battery capacity above approximately 10 kWh only resulted in marginal improvements in performance: e.g. for the 200EV case with a 500kWh supporting battery capacity, the RUF increased to 71%.

Import and Export of Electricity.

The annual electrical energy imported from the grid to the hub to support charging is shown in Figure 9. The numbers of vehicles using the hub largely dictated the energy imported from the grid. For the 10-vehicle case

¹ The EV charging profiles are generated using a probabilistic model, increases in demand will not be exact multiples of the number of vehicles.

with no battery, 85.5 kWh of imported electricity was required to support charging, whilst with 500 vehicles 7.84 MWh of electricity was imported.

As was the case with the renewable utilisation factor (RUF), a relatively small battery size of less than 10 kWh made a significant reduction to imported energy.

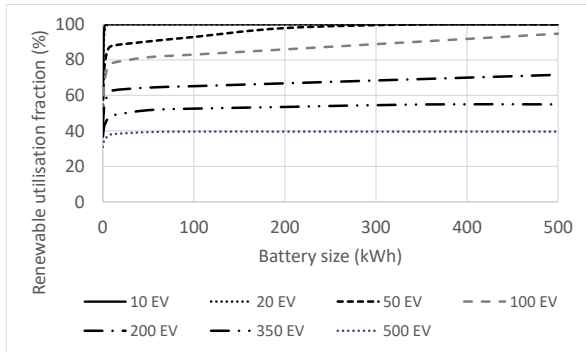


Figure 8: renewable utilisation fraction (expressed as a %) for different supporting battery sizes and vehicle fleets.

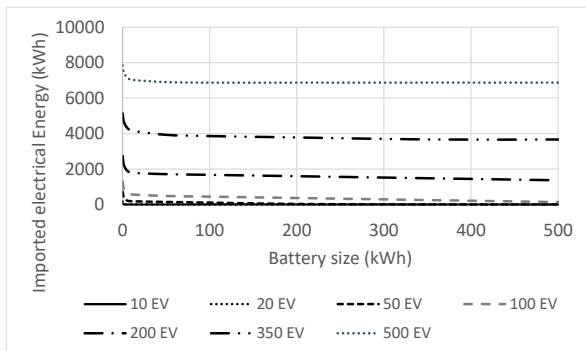


Figure 9: imported electrical energy against battery size for different vehicle fleets.

For example, with 50 vehicles using the hub, the electrical energy imported from the grid to support charging was some 0.74 MWh. Adding a 10kWh battery reduced the electricity imported to 0.19 MWh. Beyond a capacity of 10kWh, the imported energy was relatively insensitive to battery size, e.g. with a 100 kWh battery, the imported electricity was 0.11 MWh.

Figure 10 illustrates that the peak imported electrical power was only sensitive to battery size with low charging loads. At higher charging load levels, the sensitivity was minimal. The principal reason for this insensitivity is that the peak power drawn was in mid-winter when the PV contribution to charging was minimal, consequently the magnitude of power drawn was predominantly a function of the vehicle charging load.

At lower vehicle loads (< 100 vehicles) and larger battery sizes, the stored PV energy was enough to supply the vehicle charging demand throughout the year and the peak imported power (and energy) could drop to zero.

Exported electrical energy was very dependent on vehicle numbers, with increasing load from EVs reducing the exported electrical energy. As was the case with the RUF and imported energy, for a given vehicle load the annual exported energy varied markedly for battery sizes

between 1-10 kWh and was then relatively insensitive to increasing battery size. For example, with 200 vehicles using the hub, the electrical energy exported to the network was 2.50 MWh without a supporting battery; this dropped to 1.49 MWh with a battery capacity of 10 kWh and 1.02 MWh with a battery capacity of 500 kWh.

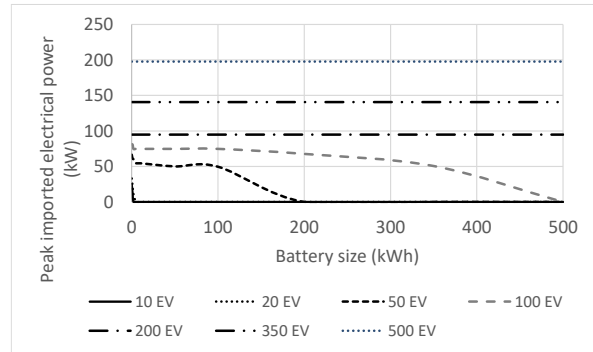


Figure 10: peak imported power against battery size for different vehicle fleets.

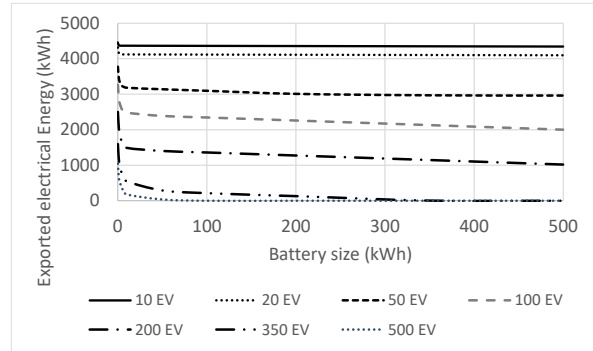


Figure 11: exported electrical energy against battery size for different vehicle fleets.

For battery sizes below 200kW, the peak exported electrical power was insensitive to the number of vehicles. Above this size, and as the number of vehicles serviced increased, the peak exported power eventually dropped to zero. In these cases, all the energy from the PV was either used to raise the battery SOC or to support vehicle charging.

Reasons for the relative insensitivity of the peak exported power value at battery sizes below 200kW were that firstly, the peak export occurred in mid-summer in the middle of the day, where the battery SOC was close to 100%, so it could absorb little of the PV generation. Secondly, with smaller numbers of vehicles, midday was a relatively quiet time for vehicle charging, so there was little EV demand to offset the PV generation. Consequently, almost all the PV peak power was exported the grid in these cases.

The battery average state of charge (SOC) over the simulated period was primarily dictated by the number of vehicles using the hub. For example, with 10 EVs, the average SOC for a 100 kWh battery was just under 100%, whilst with 200 EVs the average SOC dropped to around 38%. With 500 vehicles the average SOC was generally close to the minimum 20%, indicating that this level of

vehicle load exceeded the ability of the modelled system to support it.

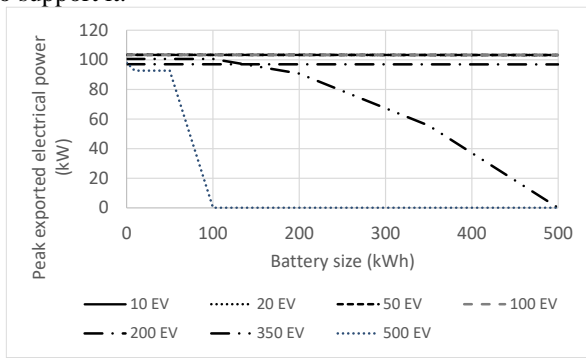


Figure 12: peak exported electrical power against battery size for different vehicle fleets.

Battery State of Charge (SOC)

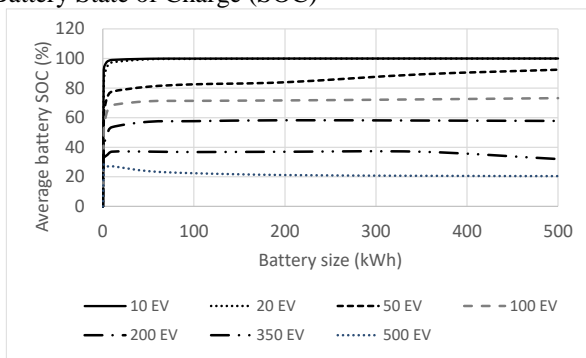


Figure 13: average battery state of charge (expressed as a %) against battery size for different vehicle fleets.

As was the case with the renewable utilisation factor and the energy imported and exported, the average SOC (for a given number of vehicles) was sensitive to smaller battery capacities (smaller than 10 kWh) and relatively insensitive to larger battery capacities. As an illustration, the average SOC for a 1 kWh battery with a hub servicing 50 EVs was 61.6%, 77.6% with the 10 kWh battery and 92.4% with a 500 kWh battery.

CONCLUSIONS

This paper has described an empirically derived electric vehicle (EV) charging model and its use to assess the value of a car-park-based photovoltaic (PV) array and a battery to support vehicle charging at a proposed charging hub in Glasgow, Scotland.

A multi-tool approach to simulating performance was employed. The ESP-r building simulation tool was used to model and simulate the performance of the PV array using real Glasgow climate data. An EV charging model was used to generate stochastic electrical charging profiles for different populations of electric vehicles serviced by the grid. A custom load flow model was used to simulate the performance of the hub.

A total of 80 cases were examined, with battery capacity (kWh) varied between 0 and 500kWh and the number of vehicles using the hub varied between 10 and 500 vehicles. The key metrics examined were the renewable utilisation factor (RUF), the energy and power exchanges with the local grid and the battery state of charge.

The peak simulated photovoltaic power output for the car park array of approximately 115 kW was significantly less than the installed PV capacity of 200 kWp and output was also strongly seasonal with very little useful power output in the winter months and a surfeit of power (for most of the cases modelled) in summer.

The renewable utilization factor (RUF) and energy exchanges with the grid (import and export) was primarily dictated by the number of EVs supported by the hub. However, the simulation results indicated that a relatively small battery capacity (10kWh or less) could make a significant difference to renewable utilization and to reduce the energy exchanges with the grid. This result also supports the findings of Mouli *et al.* 2016. Beyond this small battery capacity, only marginal gains were made in these performance metrics.

Whilst the presence of the PV and even a relatively small battery, reduced energy exchanges with the grid, their impact on peak power imported and exported from the hub was more nuanced. With less than 100 vehicles using the hub, peak power imports from the grid reduced with increasing battery size, but above this number of vehicles the battery size had a minimal effect and the peak was dictated by the number of vehicles charging. Peak exported power reduced with battery size if more than 200 vehicles used the hub, but below this load level the number of vehicles and battery size made minimal difference. Instead, the peak power exported was dictated by the size of the installed PV array.

ACKNOWLEDGEMENTS

The work reported in this paper was done as part of the RUGGEDISED EU H2020 project. Some of the algorithms used were developed under the Fabric Integrated Thermal Storage in Low Carbon Dwellings (FITS-LCD) research project. The authors gratefully acknowledge the funding provided by the EU under Grant agreement 731198 and by the EPSRC under grant EP/N021479/1, respectively. The authors also gratefully acknowledge the help and assistance of Glasgow City Council and other RUGGEDISED partners in providing key data on which this paper was based.

NOMENCLATURE

C	Capacity	kWh
e	charge on an electron	C
	(1.602177×10^{-19})	
E	Energy	kWh
F	renewable utilisation fraction	0-1
I	current	A
k	Boltzmann constant	J/K
	(1.380649×10^{-23})	
m	number of parallel connected branches	-
n	number of series connected cells in a branch	-
p	Probability	0-1 or 0-100
P	cumulative probability	0-1 or 0-100
P	power	W
q	number of panels	-

r	random value	0-1 or 0- 100
SOC	state of charge	0-1
T	Temperature	K
t	Time	s
Δt	time increment	s
V	Voltage	V
Greek Symbols		
ε	battery standing loss	0-1
λ	diode factor	-
η	efficiency	0-1

Subscripts

B	Battery	MAX	Maximum
C	Charge	OC	short circuit
c	Charging	MP	maximum power point
d	Daily	PV	Photovoltaic
D	discharge	ref	reference value
EV	electric vehicle	s	start time
G	generation current	SC	short circuit
i	layer i	t	time or time interval
L	light generated current	w	Weekly
LV	low voltage	x	Exported
MIN	Minimum	X	Converter

REFERENCES

UK Government Climate Change Act 2008 (2050 Target Amendment) Order 2019. Available at: <https://www.legislation.gov.uk/ukdsi/2019/9780111187654>. Accessed 06/05/2020.

Department for Transport, DFT, The road to zero - next steps towards cleaner road transport and delivering our Industrial Strategy, 2018, DFT report, London.

Kulagin, V. A., & Grushevenko, D. A.. Will Hydrogen Be Able to Become the Fuel of the Future? Thermal Engineering, 67, 2020, pp189-201.

Glasgow City Council, GCC, Specifications for the Duke St car park PV canopy, Glasgow City Council project report, 2018.

Earl, J., & Fell, M. J.. Electric vehicle manufacturers' perceptions of the market potential for demand-side flexibility using electric vehicles in the United Kingdom. Energy policy, 129, 2019, pp 646-652.

Bahamonde-Birke, F. J. Who will bell the cat? On the environmental and sustainability risks of electric vehicles. Transportation Research Part A: Policy and Practice, 133(C), 2020, pp 79-81.

Bhatti A R, Zainal Salam, Aziz M J B A, Yee K P, Ashique R H , Electric vehicles charging using photovoltaic: Status and technological review,

Renewable and Sustainable Energy Reviews, 54, 2016, pp34-47, ISSN 1364-0321, <https://doi.org/10.1016/j.rser.2015.09.091>.

Birnie III, D. P. Solar-to-vehicle (S2V) systems for powering commuters of the future. Journal of Power Sources, 186(2), 2009, pp 539-542.

Mouli, G. C., Bauer, P., & Zeman, M. System design for a solar powered electric vehicle charging station for workplaces. Applied Energy, 168, 2016, pp 434-443.

Tulpule, P. J., Marano, V., Yurkovich, S., & Rizzoni, G. Economic and environmental impacts of a PV powered workplace parking garage charging station. Applied Energy, 108, 2013, pp 323-332.

K. Chaudhari, A. Ukil, K. N. Kumar, U. Manandhar and S. K. Kollimalla "Hybrid Optimization for Economic Deployment of ESS in PV-Integrated EV Charging Stations," in IEEE Transactions on Industrial Informatics, vol. 14, no. 1, 2018, pp. 106-116.

D. Callaway, Tapping the energy storage potential in electric loads to deliver load following and regulation, with application to wind energy, Energy Convers. Manage., 50 (9), 2009, pp. 1389-1400

Energy Systems Research Unit, ESRU. ESP-r software: available at: <http://www.esru.strath.ac.uk/applications/esp-r/> Accessed 11/05/2020.

Strachan P, Kokogiannakis G and Macdonald I. History and Development of Validation with the ESP-r Simulation Program, Building and Environment, 43(4); 2008, pp601-609.

Kelly N J, Towards a design environment for building-integrated energy systems: the integration of power flow modelling with building simulation, PhD Thesis, 1998, University of Strathclyde, Glasgow.

Trinasolar, Datasheet TSM-PD14, ISM_EN_2016_D., 2016, Trinasolar Ltd.

Clarke J A, Hand J W, Johnstone C M, Kelly N and Strachan P A ` Photovoltaic-integrated building facades', Renewable Energy, 8(1-4), 1996, pp.475-479.

Transport Scotland, Scottish EV charge point monitoring dataset 2015-2018. Available on request.

City Parking (Glasgow). Operational performance Quarter 3. 2015, Report to Glasgow City Council. Available at: <http://www.glasgow.gov.uk/Councillorsandcommittees/viewSelectedDocument.asp?c=P62AFQUTZ3U TTINT>. Accessed 29/05/20.

Hirst D, Electric vehicles and infrastructure, House of Commons Library, 2020, Briefing Paper 7480.